Supplementary information

Title

Neuroprotection and lifespan extension in *Ppt1*$^{-/-}$ mice by NtBuHA: therapeutic implications for INCL

Authors

Chinmoy Sarkar, Goutam Chandra, Shyiong Peng, Zhongjian Zhang, Aiyi Liu and Anil B. Mukherjee

Supplementary Fig. 1 Schematic depiction of the mechanism of ceroid accumulation in INCL.

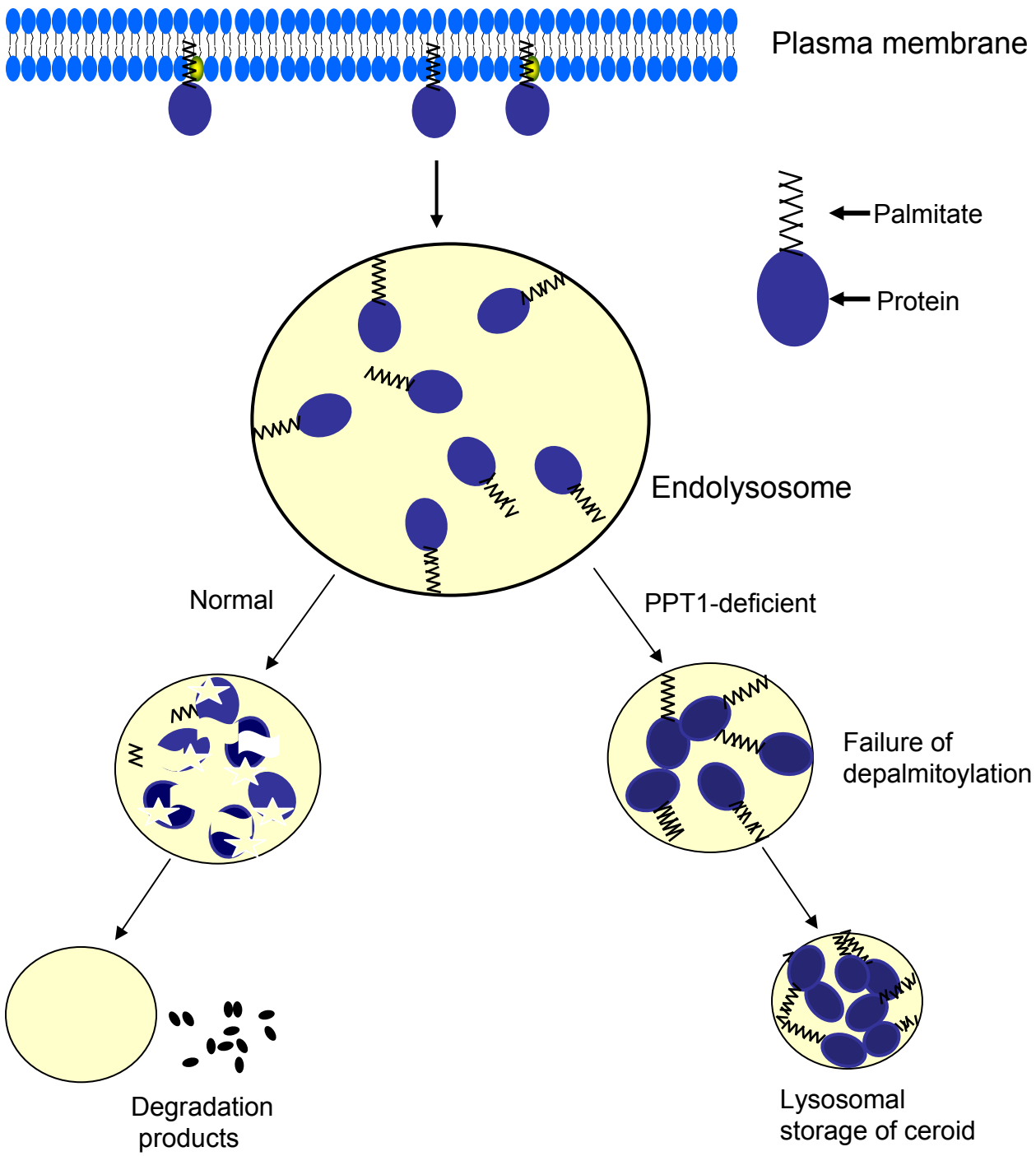

Supplementary data Fig. 1. In normal cells, the membrane-anchored palmitoylated proteins are depalmitoylated by lysosomal PPT1 and degraded by lysosomal hydrolases clearing the lysosomes. However in PPT1-deficient (INCL) cells failure of depalmitoylation makes these proteins refractory to lysosomal hydrolases. Consequently, accumulation of the palmitoylated proteins leads to lysosomal storage of ceroid causing INCL pathogenesis.

Supplementary Fig. 2. Effect of hydroxylamine derivatives on viability of INCL fibroblasts.

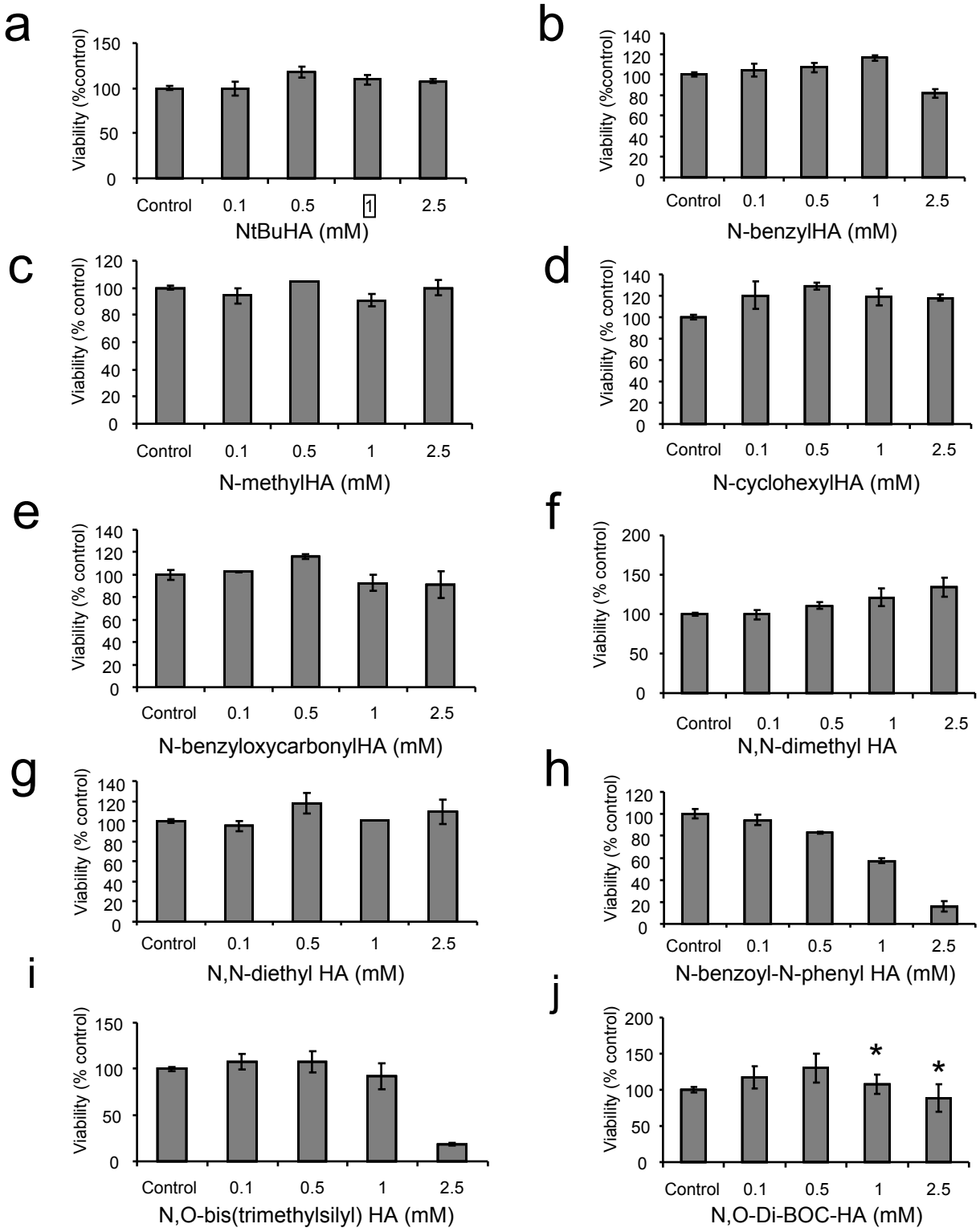

Supplementary data Fig. 2 INCL fibroblasts were incubated with increasing concentrations of **(a)** N-t-butyl hydroxylamine, **(b)** N-benzylhydroxylamine, **(c)** N-Methyl hydroxylamine, **(d)** N-cyclohexyl hydroxylamine, **(e)** N-benzyloxycarbonyl hydroxylamine, **(f)** N,N-dimethyl hydroxylamine, **(g)** N,N-diethyl hydroxylamine, **(h)** N-benzoyl-N-phenyl hydroxylamine, **(i)** N,O-bis(trimethylsilyl) hydroxylamine, **(j)** N,O-Di-BOC hydroxylamine for 48 hours. Viability of the treated cells was estimated by MTT assay (see method section). Note that most of the derivatives are nontoxic up to 1 mM concentration. * $P<0.05$.

Supplementary Fig. 3 Viability of INCL lymphoblasts treated with NtBuHA: Time Course and plating efficiency of NtBuHA treated INCL fibroblasts.

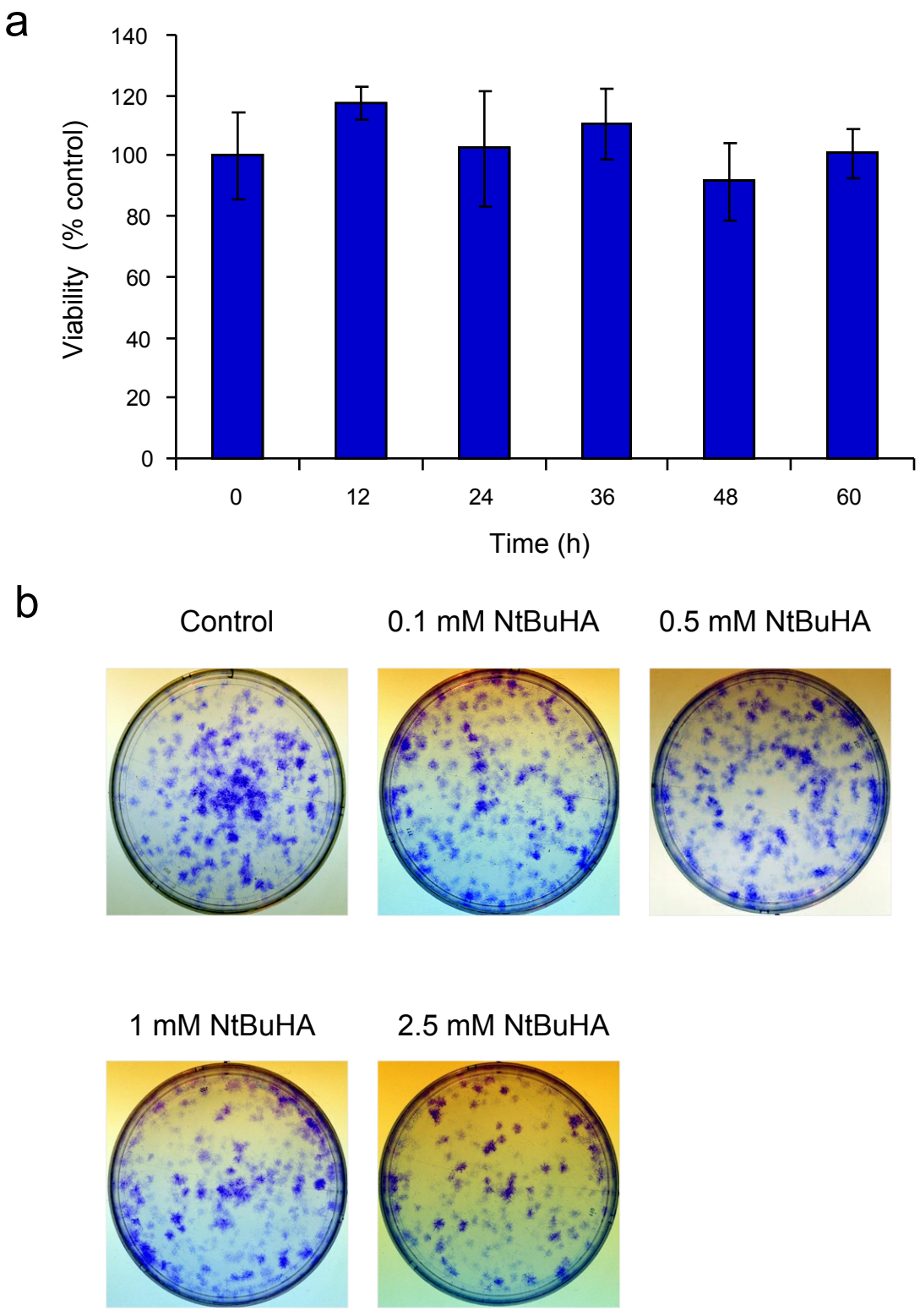

Supplementary data Fig 3. (a). Lymphoblasts isolated from INCL patients were cultured for varying length of time in presence of 500 µM NtBuHA. Viability of those cells at the end of incubation period was estimated by MTT assay and expressed as percent of viability of untreated control. The data is presented as the mean of three independent experiments ±SD. (b). Skin fibroblasts from an INCL patient were treated with varying doses (0 to 2.5 mM) of NtBuHA for 48 h. At the end of the treatment period the cells were trypsinized and re-plated at a density of 100 cells per plate. The colonies formed from 100 cells in more than 10 replicates for each treatment were stained with Crystal violet, air dried and photographed.

Supplementary Fig. 4 NtBuHA-mediated cleavage of thioester linkage in [^{14}C] Palmitoyl CoA.

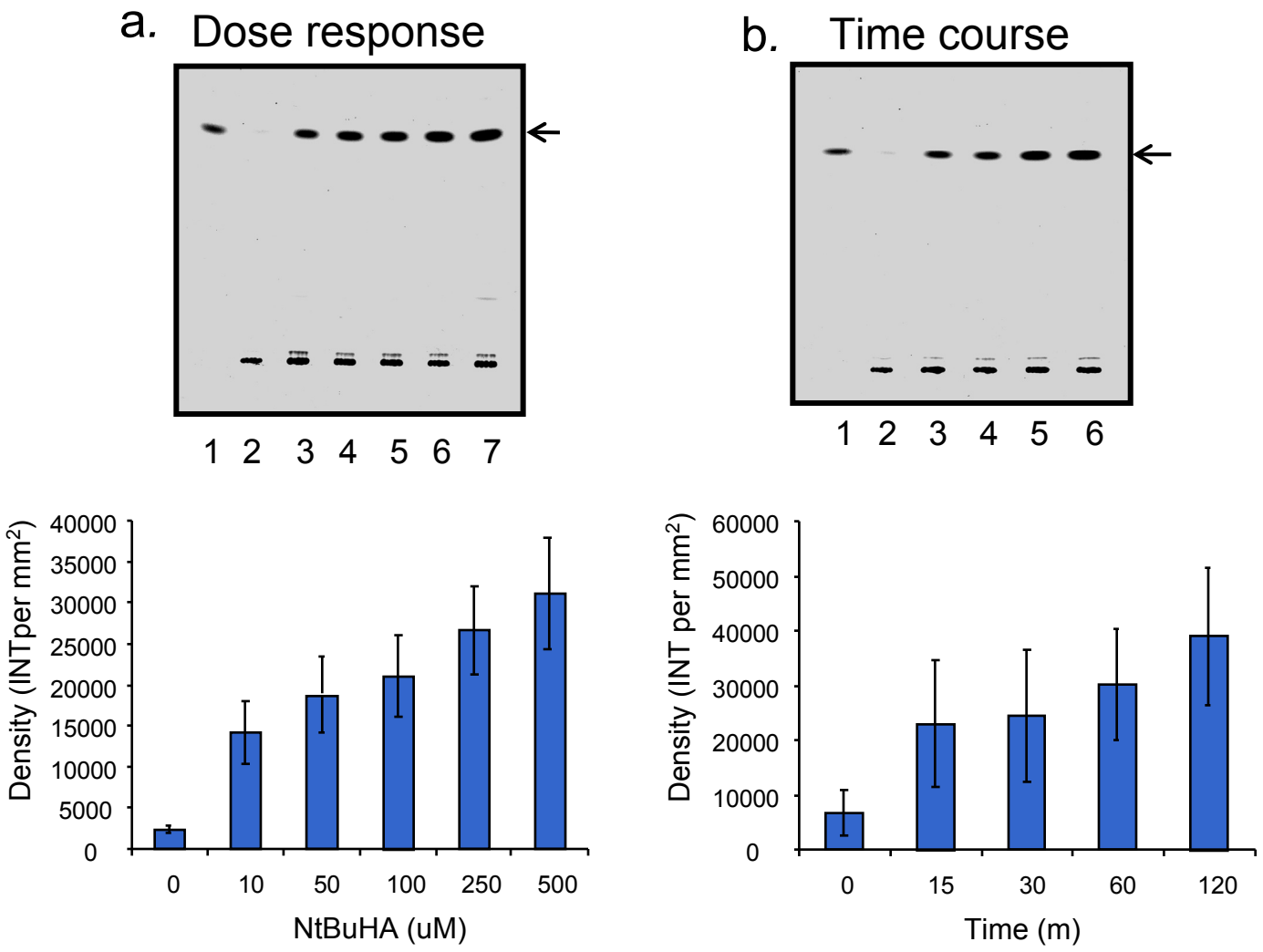

Supplementary data Fig. 4 (a) Dose-response: The release of free [^{14}C]palmitic acid from [^{14}C] palmitoyl CoA by varying doses of NtBuHA at room temperature for 1 h. **Lanes**: (**1**) [^{14}C]palmitic acid standard; (**2**) [^{14}C]-palmitoyl CoA standard; (**3**) 10 µM NtBuHA; (**4**) 50 µM NtBuHA; (**5**) 100 µM NtBuHA; (**6**) 250 µM NtBuHA and (**7**) 500 µM NtBuHA. **(b) Time-course** of [^{14}C]-palmitic acid release from [^{14}C] palmitoyl CoA by 500 µM of NtBuHA. **Lanes:** (**1**) [^{14}C]palmitic acid standard; (**2**) 0 min; (**3**) 15 min; (**4**) 30 min; (**5**) 60 min; (**6**) 120 min. Arrows indicate free [^{14}C]Palmitate released. The densitometric quantitation of free [^{14}C]palmitate bands are shown graphically below the autoradiographs of the TLCs (n=3). Note that the release of [^{14}C]palmitate from [^{14}C]-palmitoyl CoA by NtBuHA is dose- and time-dependent. The results were analyzed using student *t* test and $P<0.01$ was considered significant (in panel **a**) and $P<0.05$ in panel **b** at 60 and 120 minutes.

Supplementary Fig. 5 Densitometric quantitations of lipid thioester bands in untreated- and NtBuHA-treated INCL lymphoblasts.

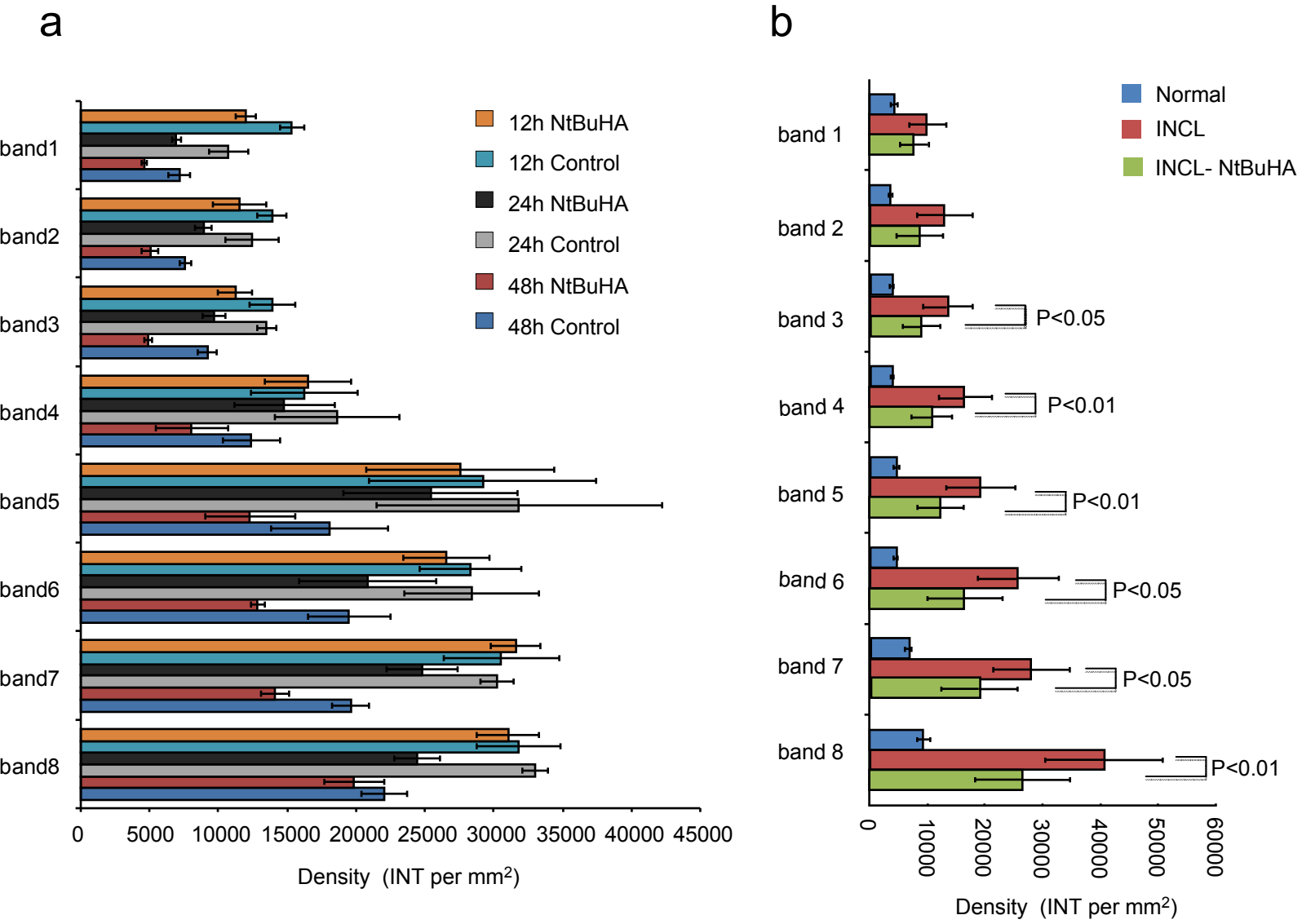

Supplementary data Fig. 5 (a). [^{35}S]Cysteine-labeled lipid thioester bands resolved by TLC as shown in Figure 1f. Eight bands were readily identifiable (arrows) and marked as bands 1 to 8 (from the top). The density of each of these bands from untreated and NtBuHA-treated INCL patients' cells were quantified using QuantityOne software (Biorad). The densitometric data are presented as the mean intensity/mm^2 (INT/mm^2) from three independent experiments ±SD. (b). [35S]Cysteine-labeled lipid thioester bands in untreated and NtBuHA-treated lymphoblasts from 9 INCL patients are resolved by TLC as shown in Figure 1g (right panel). Each of the 8 readily identifiable bands as indicated in Fig.1f was marked as bands 1 to 8 (from the top). The results of densitometric quantitation are presented as the mean of 3 independent experiments ±SD.

Supplementary Fig. 6 Depletion of GRODs in INCL fibroblasts after treatment with NtBuHA.

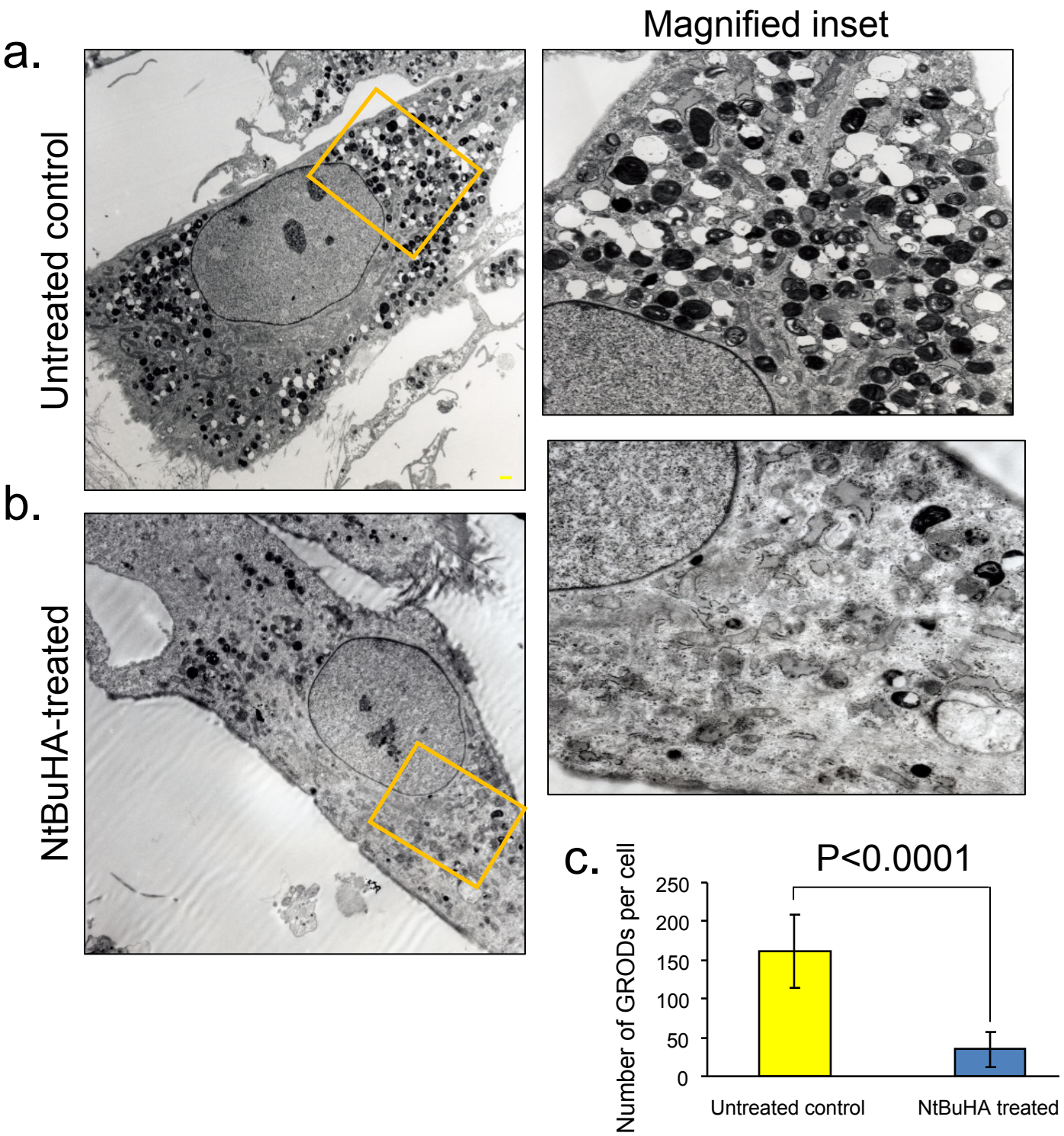

Supplementary data Fig. 6 INCL fibroblast cells were treated without (**a**) or with (**b**) 250 µM of NtBuHA for 3 weeks. Cells were then fixed in 2.5% glutaraldehyde and processed for electron microscopy. The number of GRODs/cell from untreated- (n=7) and NtBuHA-treated (n=10) INCL fibroblasts are graphically represented in panel c. Note a clear reduction in GROD level in INCL cells treated with NtBuHA. Scale bar: 1µm.

Supplementary Fig. 7 Western blot analyses of ER- and oxidative stress markers in WT and *Ppt1*$^{-/-}$ mouse brains.

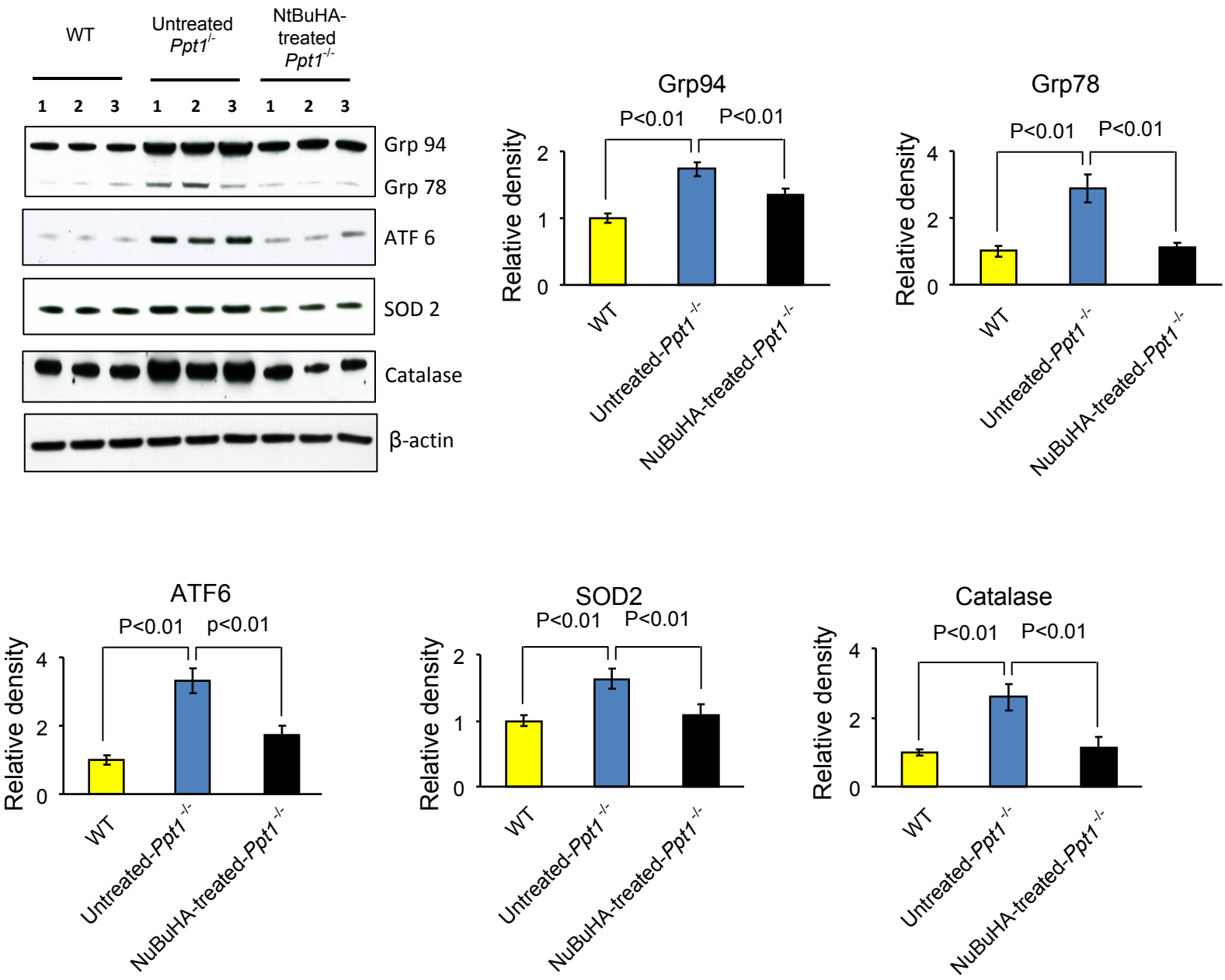

Supplementary data Fig. 7 Cortical tissue homogenates prepared from 6-month old WT, untreated-*Ppt1*$^{-/-}$ and NtBuHA-treated *Ppt1*$^{-/-}$ mice (n=6 in each group) were analyzed for ER-stress markers: ATF6, Grp94 and Grp78 and oxidative stress-markers: SOD2 and catalase, respectively. The results of densitometric quantitation of the protein bands (mean ±SDs) are represented in the bar graphs.

Supplementary Fig. 8 Protection of superficial and deep cortical neurons of *Ppt1*$^{-/-}$ mice by NtBuHA.

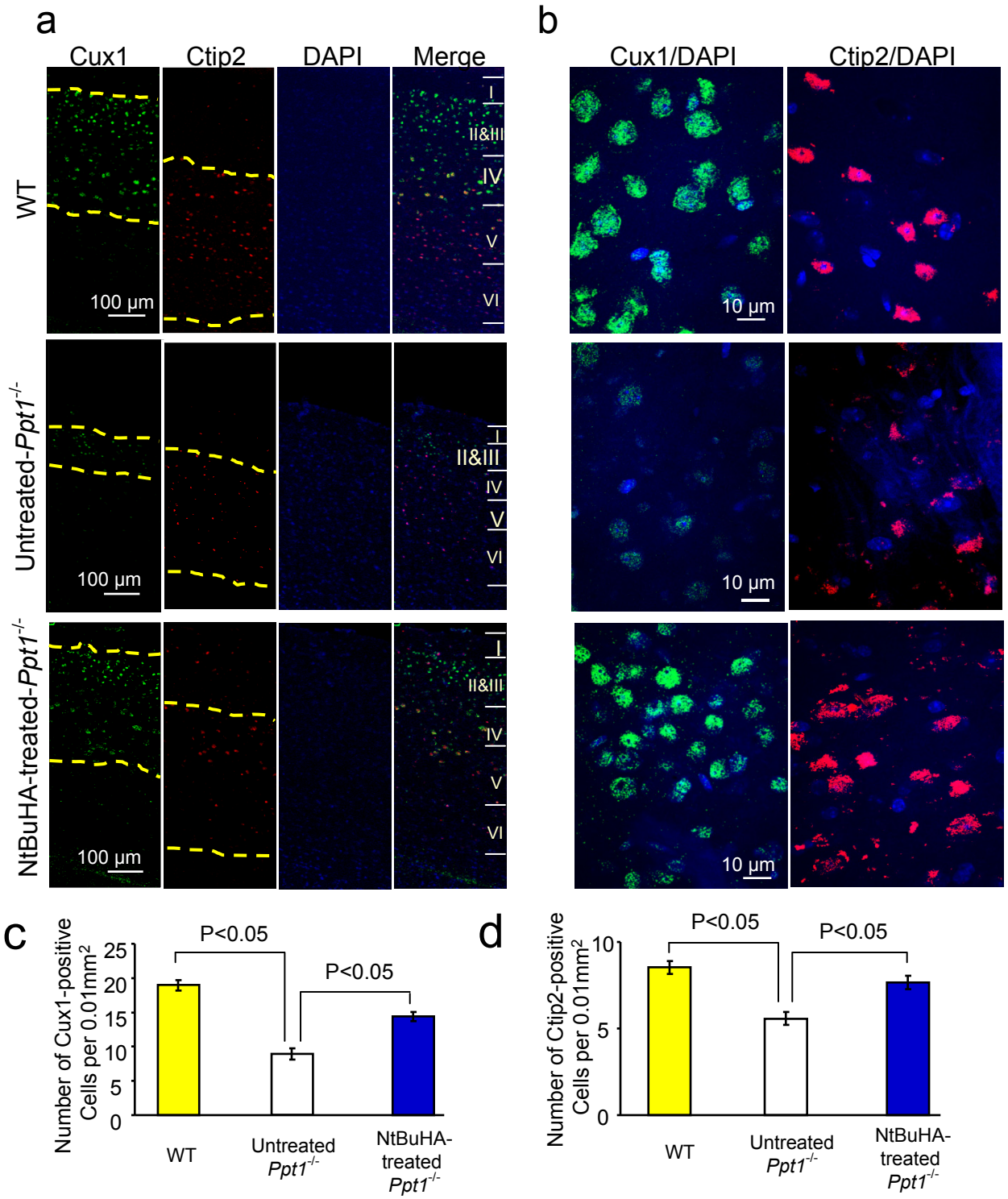

Supplementary data Fig. 8 Superficial (II-IV) and deep (IV-VI) cortical layers of WT (a; upper panel), untreated *Ppt1*$^{-/-}$ (a; middle panel), and NtBuHA-treated *Ppt1*$^{-/-}$ (a; lower panel) brain sections were immunostained with Cux1 and Ctip2 respectively. For each group, representative images of Cux1 and Ctip2 –positive cells in layers II & III and layer V respectively are shown (b). Quantification of *Cux1*- (c) and *Ctip2*- (d) positive cells per 0.01 mm^2 in these layers revealed significant protection of both these cells in NtBuHA-treated *Ppt1*$^{-/-}$ mice over their untreated littermates (n=4).

Supplementary Fig. 9 Cortical thickness in WT, untreated- and NtBuHA-treated *Ppt1*$^{-/-}$ mice; evaluation of motor coordination by rotarod rest in 3-month old WT and *Ppt1*$^{-/-}$ littermates and rotarod endurance test of untreated and NtBuHA-treated *Ppt1*$^{-/-}$ mice.

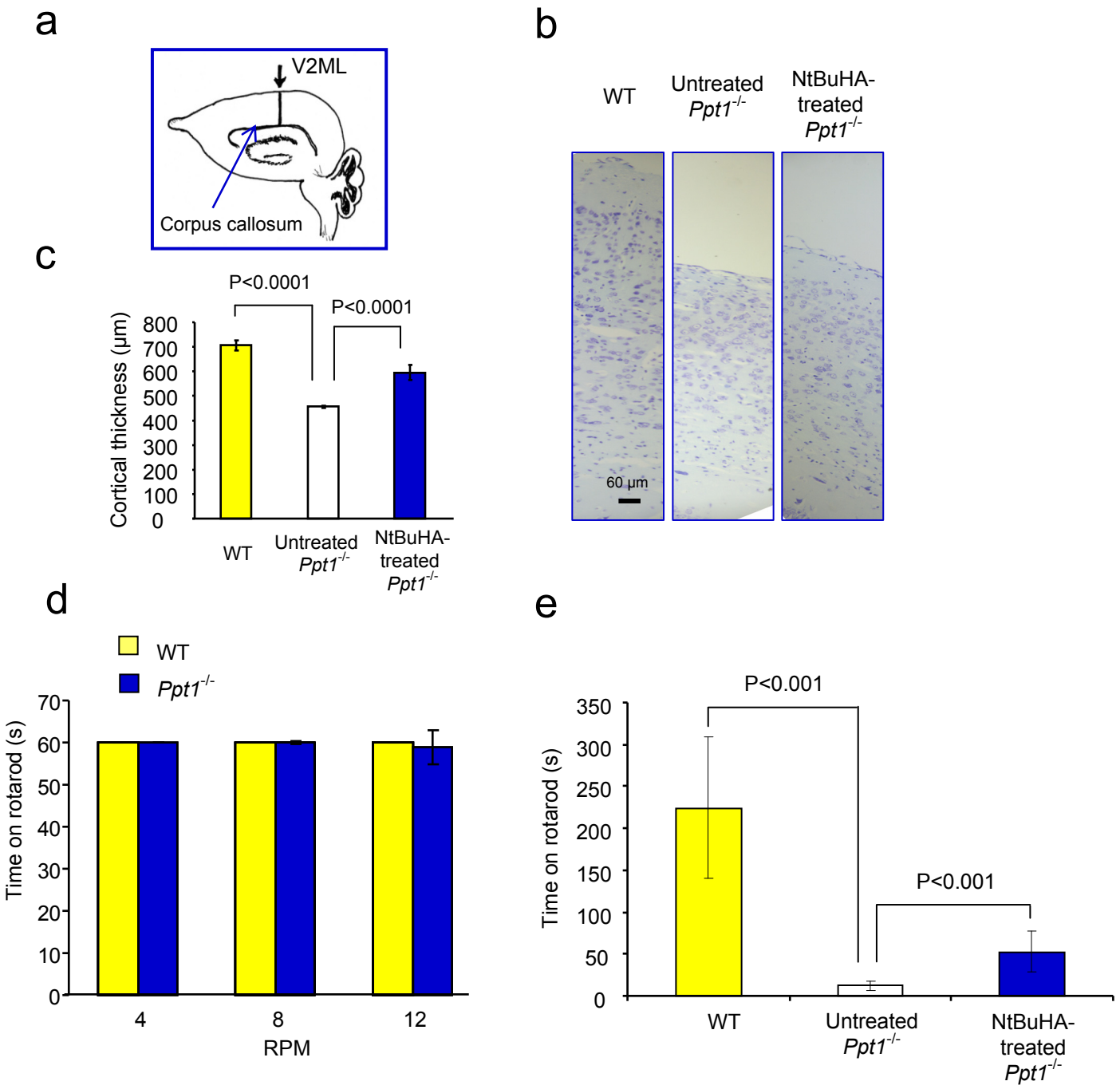

Supplementary data Fig. 9 The sections of the brain from 6-month old WT (n= 4), untreated *Ppt1*$^{-/-}$ (n=4) and NtBuHA-treated *Ppt1*$^{-/-}$ (n=4) mice were stained with cresyl violet and photomicrographs were analyzed for cortical thickness (a). Graphic representation of the brain region (V2ML, secondary visual cortex mediolateral) where the cortical thickness was measured (Arrow); (b) cresyl violet stained cortical sections from WT, untreated- and NtBuHA-treated *Ppt1*$^{-/-}$ mice; (c) graphic representation of the cortical thickness among WT mice and their untreated- and NtBuHA-treated littermates. The results are presented as the mean ± SD; (d) Three-month old WT (n=6) and *Ppt1*-/- mice (n=6) were tested on rotarod at 4, 8 and 12 rpm for 60 seconds. No significant difference in motor coordination was observed at this age between WT and *Ppt1*-/- mice; (e) Six-months old WT (n= 6), untreated *Ppt1*-/- (n=8) and NtBuHA-treated *Ppt1*-/- (n=7) mice were allowed to stay on rotarod at 12 rpm for up to 300 seconds. Note a significant, albeit modest, improvement in performance of NtBuHA-treated *Ppt1*-/- mice in the rotarod endurance test.

Supplementary Fig. 10 Full length pictures of the cropped blots presented in the main figures: 4e and 5e .

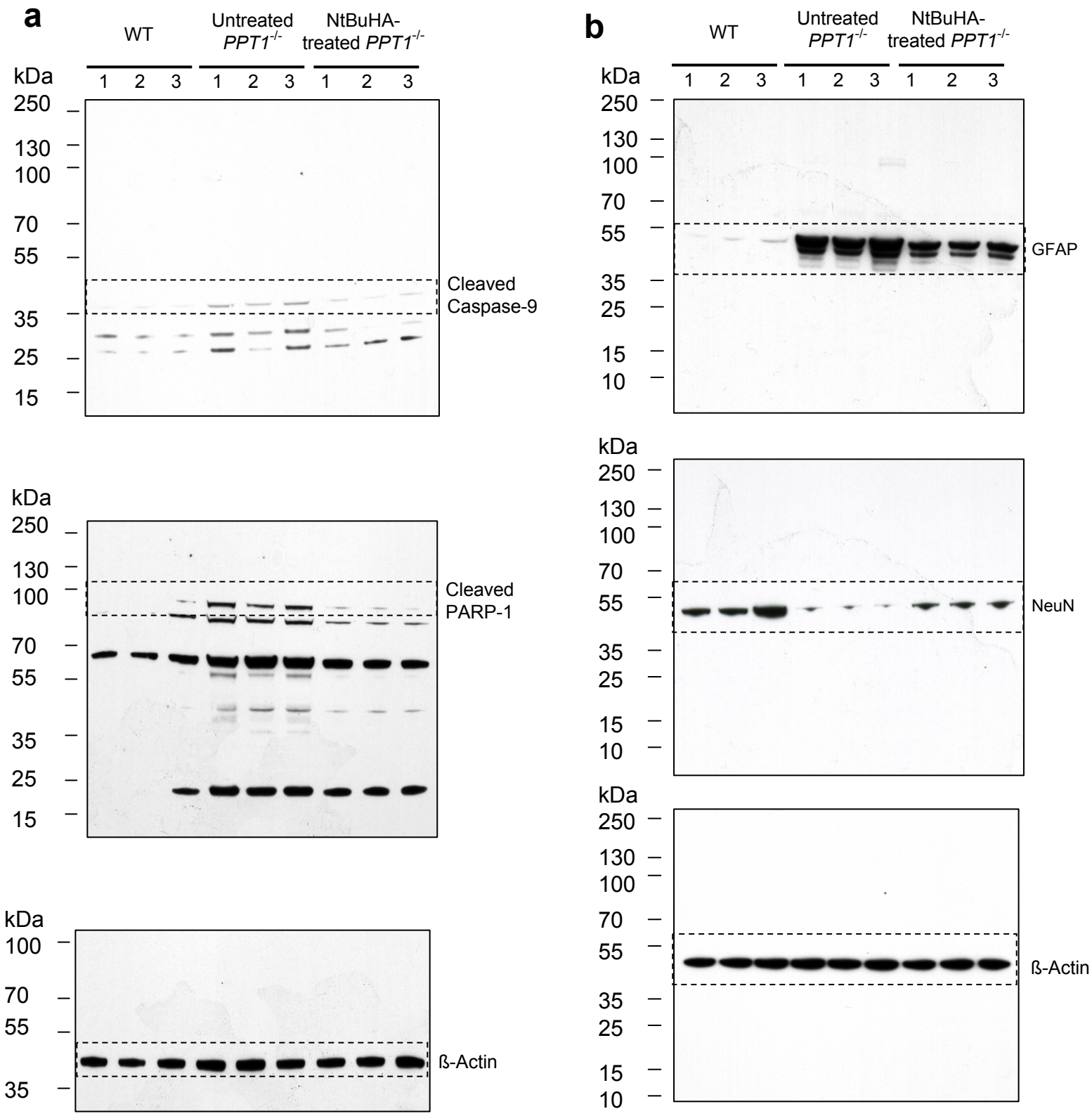

Supplementary data Fig. 10: panel a, full length picture of the cropped gel in main Figure 4e**; panel b,** full length picture of the cropped gel in main Figure 5e.

Supplemenary Table 1: Hydroxylamine and its Derivatives

	Chemical Formula	Description
	$NH_2OH \cdot HCl$	Hydroxylamine hydrochloride
1.	$C_6H_{15}NO_3$	*N*-(*tert*-Butyl)hydroxylamine acetate
2.	$C_7H_9NO \cdot HCl$	*N*-Benzylhydroxylamine hydrochloride
3.	$CH_5NO \cdot HCl$	*N*-Methylhydroxylamine hydrochloride
4.	$C_6H_{13}NO \cdot HCl$	*N*-Cyclohexylhydroxylamine hydrochloride
5.	$C_2H_7NO \cdot HCl$	*N*,*N*-Dimethylhydroxylamine hydrochloride
6.	$C_4H_{11}NO$	*N,N*-Diethylhydroxylamine
7.	$C_6H_{19}NOSi_2$	*N*,*O*-Bis(trimethylsilyl) hydroxylamine
8.	$C_8H_9NO_3$	*N*-Benzyloxycarbonyl hydroxylamine
9.	$C_{14}H_{15}NO$	*N*,*N*-Dibenzylhydroxylamine
10.	$C_{13}H_{11}NO_2$	*N*-Benzoyl-*N*-phenyl hydroxylamine
11.	$C_{23}H_{32}ClNO$	*N*-*tert*-Butyl-*O*-[1-[4-(chloromethyl) phenyl]ethyl]- *N*-(2-methyl-1-phenylpropyl) hydroxylamine
12.	$C_{10}H_{19}NO_5$	*N*,*O*-Di-Boc-hydroxylamine

Supplementary Table 2: PPT1-deficient cell lines from INCL patients

	Cell line	PPT1-mutations	
	Lymphoblasts*		
1.	C11568	Missense	A364T (R122W)
		Missense	G541A (V181M)
2.	C12275	Missense	G353A (G118D)
		Nonsense	C451T (R151X)
3.	C11796	Nonsense	C451T (R151X)
		Nonsense	C451T (R151X)
4.	C10949	Nonsense	C490T (R161X)
		Nonsense	C490T (R161X)
5.	C1045LT	Nonsense	C451T (R151X)
		Nonsense	C451T (R151X)
6.	C7142L	Nonsense	C451T (R151X)
		Missense	G541A (V181M)
7.	C10320LT	Nonsense	C451T (R151X)
		Missense	G749T (G250V)
8.	C11560	Missense	A223C (T75P)
		Nonsense	C451T (R151X)
9.	C12488	Missense	A223C (T75P)
		Missense	A223C (T75P)
10.	C9982 (N1)	Normal lymphoblasts (NL)	
11.	GM00131(N2)	Normal lymphoblasts (NL)	
12.	GM00536 (N3)	Normal lymphoblasts (NL)	
13.	C9955 (N4)	Normal lymphoblasts (NL)	
	Fibroblasts		
	INCL Fibroblasts	Missense	A364T (R122W)
		Missense	A364T (R122W)

* All lymphoblasts and their genotypes were generously provided by Late Dr. K.E. Wisniewski.

Supplemental Video: Rotarod Test

Rotarod test (60 seconds) in WT, untreated *Ppt1*$^{-/-}$ and NtBuHA-treated *Ppt1*$^{-/-}$ mice. Mouse#1 & 2 (left), NtBuHA-treated; Mouse #3 & 4 (middle), untreated and Mouse#5 (right), WT.